Check for updates

Received: 9 September 2022 | Accepted: 1 March 2023

DOI: 10.1111/ahe.12916

Anatomia Histologia Embryologia

WILEY

ORIGINAL ARTICLE

Topographic anatomy and vascularization of the glandula thyroidea in rats

Ismail Hakki Nur[1] | William Pérez[2] | Catrin Sian Rutland[3]

[1]Department of Anatomy, Faculty of Veterinary Medicine, Erciyes University, Kayseri, Turkey

[2]Unidad de Anatomia, Facultad de Veterinaria, Universidad de la Republica, Montevideo, Uruguay

[3]School of the Veterinary Medicine and Science, Faculty of Medicine and Health Sciences, University of Nottingham, Nottingham, United Kingdom

Correspondence
Ismail Hakki Nur, Faculty of Veterinary Medicine, Erciyes University, Kayseri, Turkey.
Email: hnur_55@hotmail.com

Abstract

Topographical anatomy and detailed measurements of the glandula thyroidea (thyroid gland) and the glandula parathyroidea (parathyroid gland) were determined in rats, with significant differences identified between the sexes. In the rats (N = 10 male, 10 female), the glandula thyroidea were positioned at the level of the C1 and C2 vertebrae. One glandula parathyroidea was present in each glandula thyroidea lobe, localized in the cranial part of the lateral lobes in 60% of the animals. There was no glandula thyroidea left lobe in one female and no isthmus in two females. Both the A. thyroidea cranialis and the A. pharyngea ascendens originated from the A. carotis externa, which acted as a common trunk. On the left, the A. thyroidea caudalis originated from the truncus brachiocephalicus in all rats and on the right side was found to originate from both the truncus costocervicalis and the A. subclavia dextra in three females, and only from the truncus costocervicalis in seven females. The V. thyroidea cranialis opened into the V. jugularis interna in the neck region and at the level of the apertura thoracis cranialis, and the V. jugularis interna united with the V. thyroidea caudalis. In addition, on the right, the V. thyroidea cranialis joined the V. jugularis interna, at the level of the A. subclavia. The veins on both sides opened into the V. cava cranialis. Significant differences were observed between the sexes and detailed anatomical analysis of the glandula thyroidea and the glandula parathyroidea, and related vasculature and innervation, have been described in this paper.

KEYWORDS
arteria thyroidea, glandula parathyroidea, glandula thyroidea, topographic anatomy, venae thyroidea

1 | INTRODUCTION

1.1 | Glandula thyroidea

The glandula thyroidea has long attracted the attention of the scientific world due to the number of disorders relating to it such as hypo- and hyperthyroidism. The anatomical and functional properties of this gland have not been fully elucidated and are still being investigated. The glandula thyroidea has been phylogenetically characterized as one of the oldest and largest of the endocrine glands in vertebrate species (Onwuaso & Nwagbo, 2014).

In rats, the glandula thyroidea are two-lobed structures at the C2-C3 level in Sprague-Dawley male rats, located lateral to the trachea near the base of the laryngeal cartilages (Hadie et al., 2013).

This is an open access article under the terms of the Creative Commons Attribution License, which permits use, distribution and reproduction in any medium, provided the original work is properly cited.
© 2023 The Authors. *Anatomia, Histologia, Embryologia* published by Wiley-VCH GmbH.

The guinea-pig glandula thyroidea reaches the 6th trachea ring in the caudal of the larynx (Yamasaki, 1995). The cranial margin of the glandula thyroidea is at the junction of the cricoid and thyroid cartilages. There is no correlation between the glandula thyroidea and body volumes in albino rats (Hall & Kaan, 1942). According to Nakamura et al. (2019), the glandula thyroidea may have differing volumes in the different lobes and in the rat sometimes the left lobe, or one lobe, is absent. Laterally and ventrally, the glandula thyroidea is covered by the M. sternohyoideus, immediately dorsal lies the A. carotis communis, the V. jugularis interna and the N. laryngeus caudalis (Mense & Boorman, 2018).

The glandula thyroidea has an oval cranial end and presents as a butterfly-shaped organ in the lower part of the larynx cartilages and does not join dorsal part of the trachea (La Perle et al., 2018; Tadjalli & Faramarzi, 2016; Yavru & Yavru, 1996). In rats, the glandula thyroidea is generally an oval-shaped long reddish body with smooth surfaces (Enemali et al., 2016) but in wild rats, it is long, thin and brownish, while in domesticated rats it is short, rounded and pink-red (Mosier & Richter, 1967). In the adult mongoose, the glandula thyroidea is dark brown (Tadjalli & Faramarzi, 2016). In addition, the isthmus the may not be present. For example Mota and Serkiz (2019) reported that there was no isthmus in rats, and guinea pigs do not always have one either (Yamasaki, 1995).

1.2 | Glandula parathyroidea

Although it is generally reported that rats, mice and hamsters only have one pair of glandulae parathyroidea, increased numbers have been reported in some hamsters and mice (Kittel et al., 1996b). In rats, two glandulae parathyroidea are localized in each thyroid lobe usually located bilaterally (Chiasson, 1978), under the capsule, near the dorsolateral border of each thyroid gland lobe, or on the craniolateral side of the glandula thyroidea in mice (Kittel et al., 1996b).The glandula parathyroidea can also be localized more superficial and subcapsularly. In mice, it is an oval or lens-shaped organ (Jones et al., 1983), small and variable in size (0.7–1 mm × 0.3–0.5 mm), usually at the anterolateral edge of the glandula thyroidea but this position can vary (Fox et al., 2007; Krinke, 2004). In the female mongoose, the glandula parathyroidea is positioned medial to the ventral border of the middle portion of the lobes of the glandula thyroidea, whereas in males they are in the caudal and lateral sides of each glandula thyroidea lobe (Tadjalli & Faramarzi, 2016). On the contrary, according to La perle et al. (2018) each glandula parathyroidea is rarely positioned at the same level within each individual.

In rats, the glandula parathyroidea is supplied by the same arteries that supply the glandula thyroidea (Allen & Fingeret, 2022). Therefore, there is a direct correlation between the vascular bed and the thyroid parenchyma (Abdreshov et al., 2019). In mice, the glandula parathyroidea blood supply is provided by the A. thyroidea cranialis (Murakami et al., 1987), with venous drainage provided by the V. thyroidea cranialis (Murakami et al., 1995).

1.3 | Arterial supply

The arterial blood supply for the glandula thyroidea is provided by the A. thyroidea cranialis and the A. thyroidea caudalis, both of which mainly originate from the A. carotis externa (Yamasaki, 1990). The origin of these arties has been debated in the literature but it has been reported that the A. thyroidea cranialis originates from the A. carotis externa (Stathatos, 2019) or the A. carotis interna (Monroe & Turner, 1946), whereas Vdoviaková et al. (2022) indicate that the A. thyroidea cranialis and the A. thyroidea caudalis originate from the A. carotis communis.

According to Yamasaki (1990), in more than 70% of animals, on both sides of the neck, the A. thyroidea cranialis forms a common trunk with the A. pharyngea ascendens. The main vessel feeding the glandula thyroidea, the A. thyroidea cranialis, also branches into the larynx (McLaughlin & Chiasson, 1990). The A. thyroidea caudalis is a branch of the A. subclavia, or one of its subsiduaries, and courses with the N. laryngeus caudalis (Stathatos, 2019). According to Yamasaki (1990) the A. thyroidea caudalis does not originate from the A. cervicalis profunda but instead originates from the A. phrenicopericardiaca. It has also been reported that the A. thyroidea caudalis springs from the truncus costocervicalis and the truncus cervicalis supplies the muscles of the neck and shoulder (Maynard & Downes, 2019).

Previous research has shown that the A. thyroidea cranialis gives a branch to the isthmus and anastomoses with the A. thyroidea caudalis (Green, 1955). Green (1955) also reported that the A. thyroidea caudalis runs along the lateral edge of the trachea in a cranial direction, accompanied by the N. laryngeus caudalis, and anastomoses with the A. thyroidea cranialis and terminates in the glandula thyroidea. Together, the A. thyroidea cranialis and the A. thyroidea caudalis maintain a rich anastomosis network within the glandula thyroidea (Policeni et al., 2012).

1.4 | Venous drainage

The veins originate from the glandula thyroidea parenchyma and consist of three groups of veins, the cranial, middle and caudal thyroid veins, to form a plexus alongside the V. jugularis interna and the V. brachiocephalicus (Policeni et al., 2012). The V. thyroidea cranialis and the V. thyroidea medialis in the rat glandula thyroidea open into the V. jugularis interna (Monroe & Turner, 1946). The V. thyroidea caudalis opens into the V. brachiocephalicus (Hadie et al., 2013) or the V. cava cranialis (Green, 1955).

1.5 | Innervation

Both the glandula thyroidea and the glandula parathyroidea receive their sympathetic fibres from the ganglion cervicale craniale, and their parasympathetic fibres from the N. vagus via the N. laryngeus cranialis and the N. laryngeus caudalis (Wells, 1968). In mice and

14390264, 0, Downloaded from https://onlinelibrary.wiley.com/doi/10.1111/ahe.12916 by University Of Nottingham, Wiley Online Library on [29/03/2023]. See the Terms and Conditions (https://onlinelibrary.wiley.com/terms-and-conditions) on Wiley Online Library for rules of use; OA articles are governed by the applicable Creative Commons License

rats, the sympathetic fibres are more numerous in younger individuals compared to older animals (Domeij, 1990; Kumar et al., 2018; Romeo et al., 1986).

Although there are many studies relating to the glandula thyroidea and the glandula parathyroidea anatomical structures in rats, there are no detailed studies regarding the topography of the region. In addition, to date, the circulatory and nervous systems of these regions have been depicted using hand-drawn pictures or described but not shown using photographs or corrosion casting images. This present manuscript provides topographical descriptions, measurements, and detailed anatomical images of the glandula thyroidea and the glandula parathyroidea in both male and female rats.

2 | MATERIALS AND METHODS

2.1 | Samples and perfusion

In total, 10 male and 10 female deceased Wistar albino rats, 10–11 weeks old, weighing 180–220 g, were used. The healthy rats were obtained from the Erciyes University Experimental Research and Application Center according to institutional, national and international ethical guidelines. There was no trauma, infection or drug administration present in the rats used that would affect metabolism.

The thoracic cavities of the rats were opened and 1 mL (25,000 IU) of heparin (Nevparin/Istanbul) in a 10 mL saline mixture was administered via the apex of the heart into the circulatory system until clean liquid emerged from the V. cava cranialis, thereafter processing of the latex injection and corrosion casts commenced. A digital 1/100 calliper was used for all measurements.

2.2 | Latex injections, corrosion casting and imaging

2.2.1 | Latex injection

Following perfusion, 6 mL of red latex was injected into the apex of the heart with the aid of a catheter. $N = 6$ male and 6 female rats.

2.2.2 | Corrosion cast

Following perfusion, 4 male and 4 female rats underwent corrosion casting using cold acrylic (Trade name, Takilon). Red Carmine (0.5 g, Sigma-Aldrich) was added to a mixture of powdered polymethylmethacrylate (1 g) and liquid monomethylacrylate (5 mL) and injected into the apex of the heart (Nur, 1992).

The cranial part of the body, from the level of the heart, was kept at +4°C for 24 h. The cadavers were then placed in 250 mL of distilled water with pancreatin 50 g (350 FIP-U/g protease, 6000 FIP-U/g lipase), ensuring coverage of the entire tissue. Each specimen was then incubated at 37°C and washed gently with running tap water every 4–5 h each day, after which the pancreatin water was replaced. The soft tissues were removed within 3 days, and images were taken following natural drying.

2.2.3 | Imaging

Images were acquired using a Zoom Stereomicroscope (Olympus SZ-PT-Japan- Auxiliary objective 100ALO 0.5X, eyepiece GSWH 10X/22) with a SAMSUNG NX300-Japan, 20.3 MP camera to capture photomicrographs. Terminology is based on Nomina Anatomica Veterinaria (I.C.V.G.A.N., 2017).

2.2.4 | Statistics

Statistical analysis was conducted using SPSS v26.0 (IBM Corporation). Levene's test for Equality of Variances was undertaken, and all data were normally distributed; therefore, independent samples *t*-tests were conducted, and significance was determined at $p > 0.05$. Statistical analysis was conducted for all quantitative measurements which included the glandula thyroidea weight, right and left lobe length, width and breadth (termed thickness), right cranial and caudal pole widths, and the isthmus length, width and breadth (thickness), and the glandula parathyroidea length and width, alongside the diameters of the A. thyroidea cranialis, A. thyroidea caudalis, V. thyroidea cranialis, V. thyroidea caudalis, V. jugularis interna and the A. carotis communis.

3 | RESULTS

3.1 | Glandula thyroidea, glandula parathyroidea, isthmus and vascular measurements, anatomical locations and appearance

In the study, both the borders of the glandula thyroidea and its relationship with the anatomical structures in the region were investigated. The measurements created using the latex and corrosion casting, and accompanying statistical analysis, are provided in Table 1.

3.2 | Topographic anatomy of the glandula thyroidea

In the supine position, the skin was cut along the median line from the apertura thoracis cranialis to the chin; then, the skin and underlying connective tissue were removed. The muscles on the ventral aspect of the neck were also exposed, and the glandula mandibularis and the nodus lymphoideus mandibularis were carefully removed. The M. sternohyoideus and the M. sternomastoideus extending laterally were observed in the ventromedial region of the trachea. The M. omohyoideus was determined as the broad band extending from the ventral edge

14390264, 0, Downloaded from https://onlinelibrary.wiley.com/doi/10.1111/ahe.12916 by University Of Nottingham, Wiley Online Library on [29/03/2023]. See the Terms and Conditions (https://onlinelibrary.wiley.com/terms-and-conditions) on Wiley Online Library for rules of use; OA articles are governed by the applicable Creative Commons License

TABLE 1 Measurements of the glandula thyroidea and the glandula parathyroidea in Wistar albino rats ($n = 5$/sex).

Measurement (mm)	Male ($n = 5$)	Female ($n = 5$)	p Value (male vs. female)
Glandula thyroidea right lobe length	4.34 ±0.02	4.02 ±0.08	**0.001**
Glandula thyroidea left lobe length	4.30 ±0.01	4.11 ±0.06	**0.0001**
Glandula thyroidea right lobe width	1.87 ±0.07	1.68 ±0.03	**0.001**
Glandula thyroidea left lobe width	1.85 ±0.05	1.60 ±0.01	**0.0001**
Glandula thyroidea right lobe thickness	0.86 ±0.02	0.80 ±0.01	**0.0001**
Glandula thyroidea left lobe thickness	0.82 ±0.02	0.80 ±0.01	0.056
Right cranial pole—glandula thyroidea width	3.80 ±0.09	3.78 ±0.02	0.793
Right caudal pole—glandula thyroidea width	3.62 ±0.03	3.50 ±0.03	**0.001**
Isthmus length	3.21 ±0.03	3.12 ±0.02	**0.001**
Isthmus width	1.86 ±0.03	1.70 ±0.07	**0.003**
Isthmus thickness	0.33 ±0.02	0.21 ±0.02	**0.0001**
Glandula parathyroidea length	1.22 ±0.03	0.95 ±0.06	**0.0001**
Glandula parathyroidea width	1.02 ±0.07	0.86 ±0.04	**0.002**
A. thyroidea cranialis diameter	0.29 ±0.02	0.25 ±0.02	**0.003**
A. thyroidea caudalis diameter	0.20 ±0.01	0.22 ±0.02	**0.049**
V. thyroidea cranialis diameter	0.21 ±0.01	0.20 ±0.01	0.291
V. thyroidea caudalis diameter	0.34 ±0.02	0.27 ±0.04	**0.011**
V. jugularis interna diameter	0.26 ±0.01	0.23 ±0.02	0.071
A. carotis communis diameter	0.82 ±0.03	0.76 ±0.02	**0.007**
Glandula thyroidea weight (grams)	0.0066 ±0.0037	0.0055 ±0.0022	0.575

Note: Numbers represent mean ± standard deviation. Significant differences are indicated in bold.

of the scapula to the basihyoideum, in the ventrolateral side of the glandula thyroidea. The M. sternothyroideus was located under the M. sternohyoideus and advanced to the craniolateral side of the trachea like a band with a thickness of approximately 1.00 ± 0.15 mm.

The rat glandula thyroidea weights did not differ between males and females at 6.6 ± 3.7 mg in males and 5.5 ± 2.2 mg in females (Table 1; $p > 0.575$), despite most of the length, width and thickness measurements being significantly larger in males (Table 1; $p < 0.05$). Each glandula thyroidea was a reddish-brownish coloured organ consisting of two lobes connected by a narrow isthmus, located ventrolateral to the trachea just behind the larynx. The glandula thyroidea was located at the C1 and C2 vertebral levels in both male and female Wistar albino rats. The glandula thyroidea consisted of two lobes (the lobus dexter and the lobus sinister).The cranial ends of the glandulae thyroidea were pointed. It also extended to the caudolateral edge of the cartilago thyroidea. The caudal ends of the glandulae thyroidea extended to the level of the 3rd or 4th cartilage rings of the trachea, forming a blunter shape compared to the cranial ends.

In rats, the lobus dexter and lobus sinister did not converge dorsal to the trachea; there was no lobus sinister present in one female. The lobus dexter and the lobus sinister were connected together by a thin, narrow and transparentisthmus (Figures 1–3). The transparent nature of the isthmus made it difficult to identify but it was positioned at the level of 1st and 2nd trachea ring. There was no isthmus present in two females.

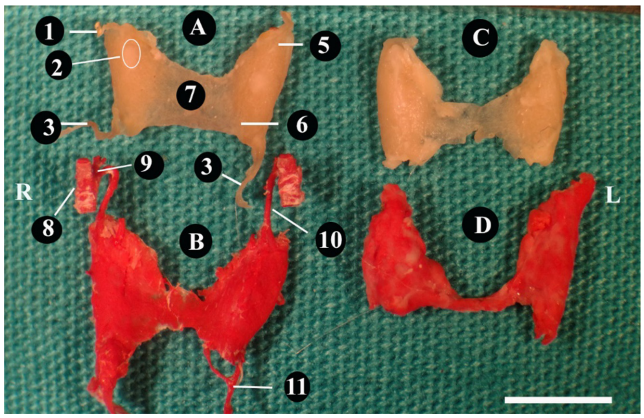

FIGURE 1 Glandula thyroidea and the glandula parathyroidea. Ventral view. (a, b) Male, normal tissue and with injected latex, (c, d) Female, normal tissue and with injected latex. 1. N. laryngeus cranialis, 2. Glandula parathyroidea, 3. N. laryngeus caudalis, 5. Cranial end of the glandula thyroidea, 6. Caudal end of the glandula thyroidea, 7. Isthmus, 8. A. carotis externa, 9. A. pharyngea ascendens, 10. A. thyroidea cranialis, 11. A. thyroidea caudalis. Scale bar = 4 mm.

Following the removal of the M. omohyoideus and the M. sternohyoideus, the vascular nerve bundle in this region was easily visualized. The bundle, from medial to lateral, contained the A. carotis communis (medial side), the truncus symphaticus

14390264, 0, Downloaded from https://onlinelibrary.wiley.com/doi/10.1111/ahe.12916 by University Of Nottingham, Wiley Online Library on [29/03/2023]. See the Terms and Conditions (https://onlinelibrary.wiley.com/terms-and-conditions) on Wiley Online Library for rules of use; OA articles are governed by the applicable Creative Commons License

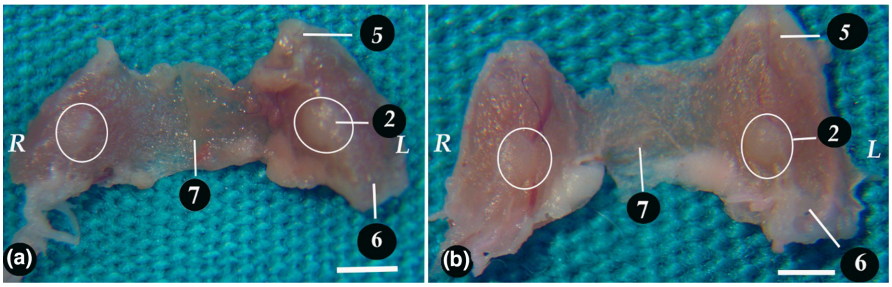

FIGURE 2 Glandula thyroidea, the glandula parathyroidea and the isthmus. Ventral view. (a) Male, (b) Female. R. Right, L. Left. 2. Glandula parathyroidea, 5. Cranial end of the glandula thyroidea, 6. Caudal end of the glandula thyroidea, 7. Isthmus. Scale bar = 1 mm.

(dorsolateral side), the V. jugularis interna (posterior side) and the N. vagus (lateral side).

In both sexes, 60% of the glandulae parathyroidea was situated on the lobus dexter and sinister, while 30% was at the level of the isthmus, and 10% was in the ventrolateral part of the lateral lobe. The glandula parathyroidea and glandula thyroidea both had dense vascular networks.

3.3 | Blood supply and innervation of the glandula thyroidea

The glandula thyroidea arterial blood supply consisted of branches of the A. carotis communis, the main branch was the A. thyroidea cranialis, and the A. thyroidea caudalis, which supplied the larynx and theglandula parathyroidea. Venous circulation of the glandula thyroidea and the glandula parathyroidea was carried out through the V. thyroidea cranialis and the V. thyroidea caudalis, similar to that observed in the arterial system. The glandula thyroidea was innervated by both the sympathetic and parasympathetic nervous systems. A thin capsule covering the glandula thyroidea containing both the vessels and nerves was observed.

3.3.1 | Arterial supply of the glandula thyroidea

The A. carotis communis had significantly smaller diameters in females compared to males (Table 1; $p = 0.007$). The A. thyroidea cranialis originated from the A. carotis communis below the venter caudalis of the M. digastricus, at the level of the upper end of the ganglion cervicale cranialis. Moreover, it was determined that it originated from a common root with the A. pharyngea ascendens in five females and six male rats. After the A. thyroidea cranialis origin, it divided into two presenting as dorsal and ventral branches. The ventral branch was larger in diameter than the dorsal branch. The ventral branch then divided into two dorsal and ventral end branches after its origin, and the dorsal branch of ventral branch terminated in the upper part of the lateral lobe of the glandula thyroidea. Meanwhile, the ventral branch of the ventral branch extended from the lateral edge of the glandula thyroidea to the ventral edge and anastomosed with the A. thyroidea caudalis. The dorsal branch gave branches to the larynx muscles and the beginning of the oesophagus on the dorsal surface of the trachea (Figures 4–7).

The A. thyroidea caudalis was positioned on the dorsolateral part of the N. laryngeus caudalis on both sides. The origins of the

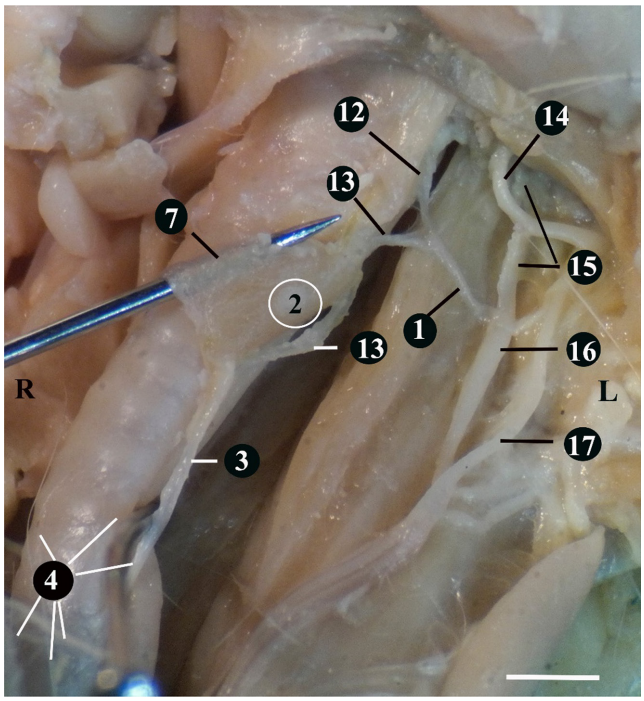

FIGURE 3 Sympathetic and parasympathetic nerves serving the glandula thyroidea and the glandula parathyroidea. Ventral view. R. Right side, L. Left side. 1. N. laryngeus cranialis, 2. Glandula parathyroidea 3. N. laryngeus caudalis, 4. N.laryngeus reccurens and its tracheal branches, 7. Isthmus, 12. N. laryngeus cranialis and its laryngeal branch, 13. N. laryngeus cranialis and its thyroid branch, 14. N. hypoglossus, 15. Ganglion cervicale craniale, 16. Truncus symphaticus, 17. N. vagus. Scale bar = 1 mm.

A. thyroidea caudalis on the right and left sides differed from each other. On the right side, the A. thyroidea caudalis was found to originate from both the truncus costocervicalis and the A. subclavia in three females, and only from the truncus costocervicalis in the remaining seven females. On the left side, the A. thyroidea caudalis originated from the truncus brachiocephalicus at the beginning of the A. carotis communis in the rats.

Following the course of the A. thyroidea caudalis showed that it extended to the glandula thyroidea with the N. laryngeus caudalis in the *tracheoesophageal sulcus* on both sides and entered the glandula thyroidea from the ventral ends of the lobes. It was determined that the A. thyroidea caudalis, on both sides, gave rise to thin branches for both the oesophagus and the tracheal rings at the level of each ligg. anularia of the trachea. Both the A. thyroidea cranialis and the A. thyroidea caudalis had significantly larger diameters in males compared to females (Table 1; $p < 0.05$).

14390264, 0, Downloaded from https://onlinelibrary.wiley.com/doi/10.1111/ahe.12916 by University Of Nottingham, Wiley Online Library on [29/03/2023]. See the Terms and Conditions (https://onlinelibrary.wiley.com/terms-and-conditions) on Wiley Online Library for rules of use; OA articles are governed by the applicable Creative Commons License

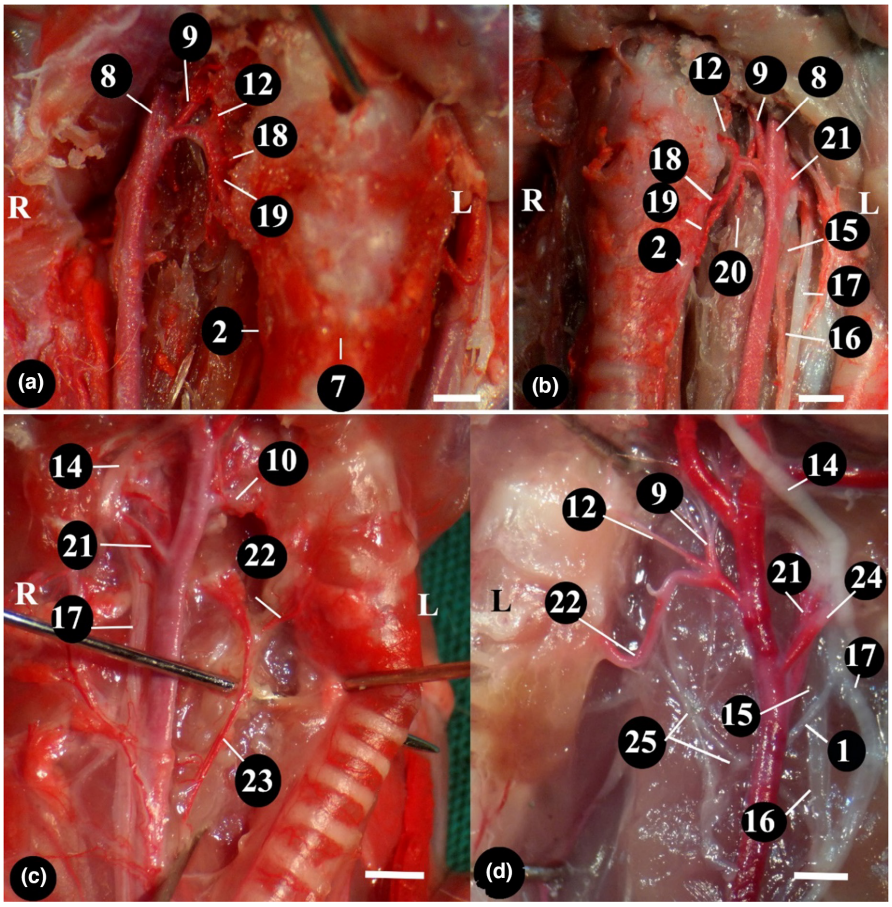

FIGURE 4 A. thyroidea cranialis and its branches. Ventral and Ventrolateral view. (a) (b) Male, (c, d) Female, R. Right, L. Left. 1. N. laryngeus cranialis, 2. Glandula parathyroidea, 7. Isthmus, 8. A. carotis externa, 9. A. pharyngea ascendens, 10. A. thyroidea cranialis, 12. A. thyroidea cranialis and its laryngeal branch, 14. N. hypoglossus, 15. Ganglion cervicale craniale, 16. Truncus symphaticus, 17. N. vagus, 18. A. thyroidea cranialis and its cranial branch, 19. A. thyroidea cranialis and its caudal branch, 20. A. thyroidea cranialis and its muscular branch, 21. A. carotis interna, 22. V. thyroidea cranialis, 23. V. jugularis interna, 24. A. occipitalis, 25. Sympathetic branches of ganglion cervicale craniale. Scale bar = 1 mm.

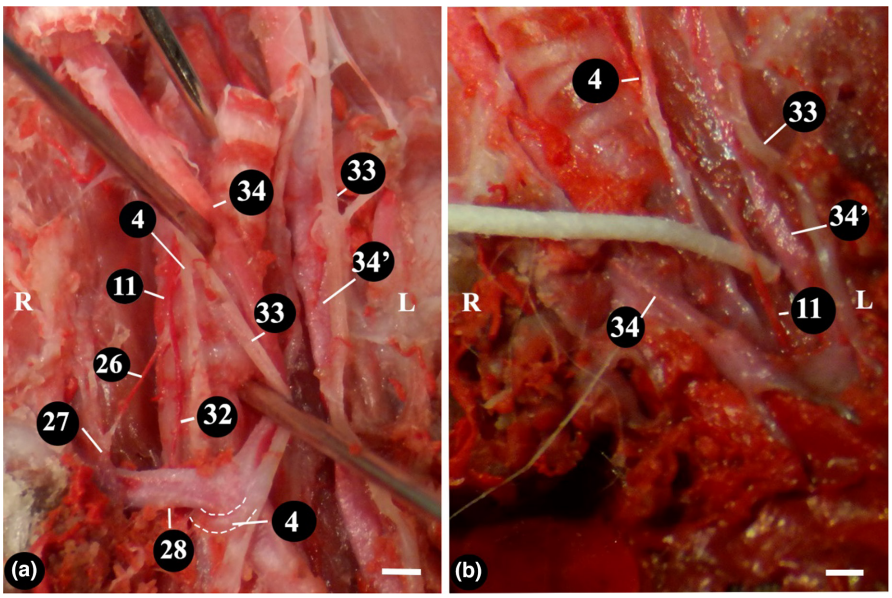

FIGURE 5 Origin of the A. thyroidea caudalis. Ventral view. Female rat. R. Right, L. Left. 4. N. laryngeus reccurens, 11. A. thyroidea caudalis, 26. A branch of the A. thyroidea caudalis originating from the truncus costocervicalis, 27. Truncus costocervicalis, 28. A. subclavia dextra, 32. Another branch of the A. thyroidea caudalis which originated from the A. subclavia dextra, 33. Truncus vagosympathicus, 34, 34′. A. carotis communisdextra et sinistra. Scale bar = 1 mm.

3.3.2 | Venous drainage

The origin and course of the V. thyroidea cranialis and the V. thyroidea caudalis on the right and left differed from each other (Figures 8–10). On the right side, the V. thyroidea cranialis originated from the cranial part of the glandula thyroidea lobe, and the V. thyroidea caudalis originated from the caudal part of the glandula thyroidea. After the origin of the V. thyroidea cranialis on both sides of the neck, each opened into the V. jugularis interna. The V. jugularis interna reached the ventral surface of the N. vagus after a short course, and these two anatomic structures were contained within the same connective tissue sheath. Then, the V. jugularis interna united with the V. thyroidea caudalis at the subclavian artery level. Thereafter, it opened into the V. subclavian dextra as a single vessel.

14390264, 0, Downloaded from https://onlinelibrary.wiley.com/doi/10.1111/ahe.12916 by University Of Nottingham, Wiley Online Library on [29/03/2023]. See the Terms and Conditions (https://onlinelibrary.wiley.com/terms-and-conditions) on Wiley Online Library for rules of use; OA articles are governed by the applicable Creative Commons License

On the left side, the V. thyroidea cranialis opened into the V. jugularis interna. The V. thyroidea caudalis originated from the caudal end of the lobus sinister and opened 1 cm later into the V. jugularis interna at the level of the apertura thoracis cranialis. The V. jugularis interna also opened to the V. cava cranialis.

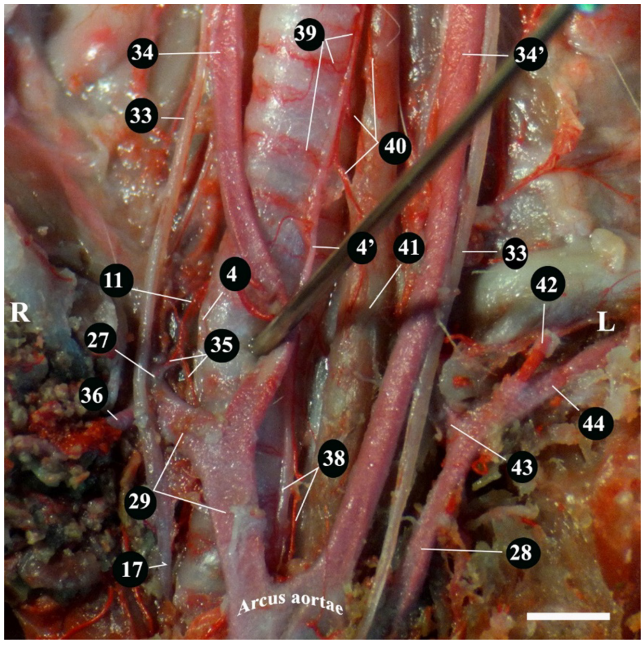

FIGURE 6 Origin of the thyroid arteries. Ventral view. Female rat. R. Right, L. Left. 4,4′. N. laryngeus reccurens dexter and sinister, 11. A. thyroidea caudalis (dexter), 17. N. vagus, 27. Truncus costocervicalis (dexter), 28. A. subclavia sinistra, 29. A. subclavia dextra and truncus brachiocephalicus, 33. Truncus vagosympathicus, 34, 34′. A. carotis communis dextra et sinistra, 35. Branches originating from the truncus costocervicalis and the A. subclavia dextra to form the A. thyroidea caudalis, 36. A. axillaris, 38. A. thyroidea caudalis (sinister) and N. laryngeus reccurens (sinister), 39. A. thyroidea caudalis (sinister) and its tracheal branches, 40. A. thyroidea caudalis (sinister) and its oesophageal branches, 41. Oesophagus, 42. A. cervicalis profunda, 43. A. vertebralis, 44. A. intercostalis suprema. Scale bar = 1 mm.

The V. thyroidea caudalis was larger diameter in males compared to females (Table 1; $p = 0.011$), whereas no sex differences were observed between the diameters of the cranial veins in relation to the sexes (Table 1; $p = 0.291$).

3.4 | Innervation

Parasympathetic innervation of the glandula thyroidea in the cadavers was provided by the N. laryngeus cranialis and the N. laryngeus caudalis, the terminal branch of the N. laryngeus reccurens (Figures 3–5, 8 and 10). It was determined that the sympathetic threads were provided by the branches coming from the ganglion cervicale craniale, both to the tissue of the gland and the network which formed around the vessels.

The N. laryngeus cranialis was separated from the N. vagus on the lateral edge of the ganglion cervicale craniale. After its origin, it followed the A. thyroidea cranialis, passing through the ventral edge of the ganglion cervicale craniale and dorsal of the A. carotis communis. The N. laryngeus cranialis divided into the internal (dorsal) and external (ventral) two branches at the level of the ventral branch of the A. thyroidea cranialis. It was determined that the dorsal branch entered the larynx mucosa, and the ventral branch terminated in the M. cricothyroideus and the lateral lobe of the glandula thyroidea.

The N. laryngeus caudalis was the termination of the N. laryngeus reccurens. There are two recurrent laryngeal nerves, right and left. The right and left nerves were not symmetrical. The N. laryngeus reccurens originated from the N. vagus at the thoracic inlet. On the left, the N. laryngeus reccurens looped under the arcus aortae. On the right, it looped under the A. subclavia dextra. Then, each N. laryngeus reccurens coursed along the tracheoesophageal sulcus towards the head. It progressed together with the N. laryngeus reccurens, the V. thyroidea caudalis, and the A. thyroidea caudalis on both sides, and the vessels and nerves were laterally covered by the M. sternothyroideus.

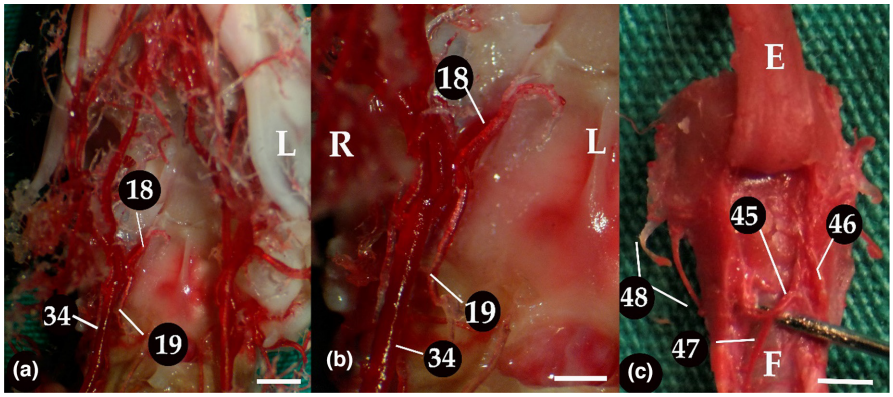

FIGURE 7 Corrosion casts of the vasculature and anastomosis. Male rat. R. Right, L. Left, E. Oesophagus, F. Trachea. (a, b) Ventral view, (c) Dorsal view. 18. Cranial branch of the A. thyroidea cranialis, 19. Caudal branch of the A. thyroidea cranialis, 34. A. carotis communis dextra, 45. Anastomosis between A. thyroidea cranialis and A. thyroidea caudalis, 46. Dorsal branch of the A. thyroidea cranialis, 47. Dorsal branch of the A. thyroidea caudalis, 48. N. laryngeus cranialis and the A. thyroidea cranialis. Scale bar = 1 mm.

14390264, 0, Downloaded from https://onlinelibrary.wiley.com/doi/10.1111/ahe.12916 by University Of Nottingham, Wiley Online Library on [29/03/2023]. See the Terms and Conditions (https://onlinelibrary.wiley.com/terms-and-conditions) on Wiley Online Library for rules of use; OA articles are governed by the applicable Creative Commons License

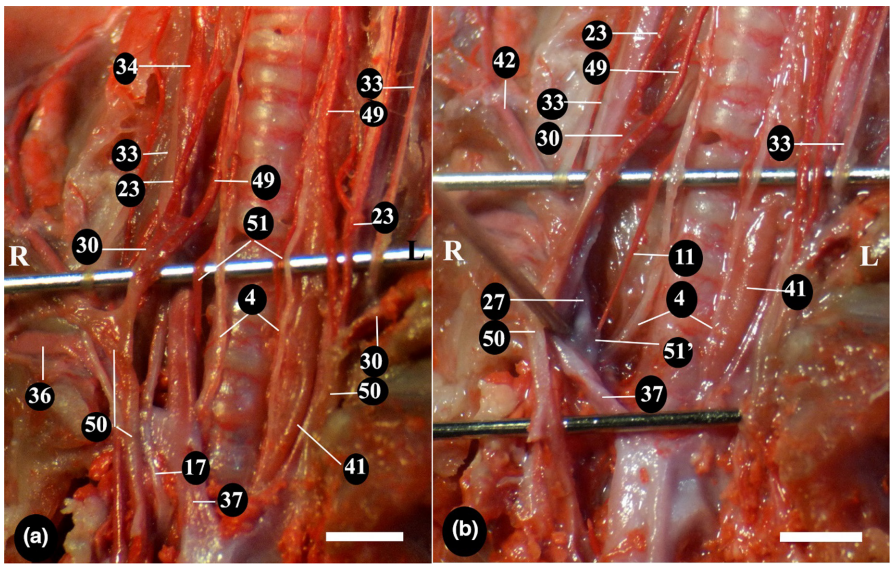

FIGURE 8 Origin of A. thyroidea caudalis and venous drainage of the glandula thyroidea. Ventral view. Male rat. R. Right, L. Left. 4. N. laryngeus reccurens, 11. A. Thyroidea caudalis, 17. N.vagus, 23. V. jugularis interna, 27. Truncus costocervicalis, 30. V. subclavia (dextra) at the junction of the V. thyroidea caudalis and the V. jugularis interna, 33. Truncus vagosympathicus, 34. A. carotis communis dextra, 36. A. axillaris, 37. Truncus brachiocephalicus. 41. Oesophagus, 42. A. cervicalis profunda, 49. V. thyroidea caudalis, 50. V. cava cranialis, 51. A. thyroidea caudalis, 51′. Origin of A. thyroidea caudalis (dexter). Scale bar = 1 mm.

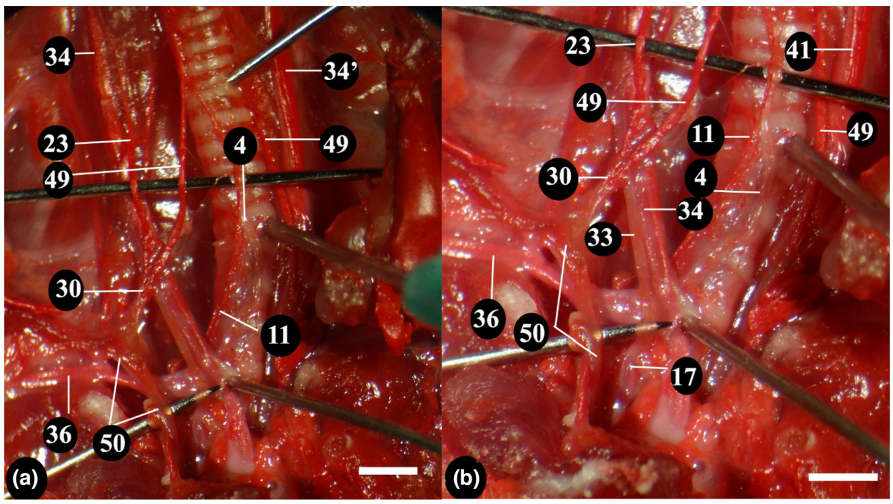

FIGURE 9 Venous drainage. Ventral view. Male rat, R. Right, L. Left. 4. N. laryngeus reccurens, 11. A. thyroidea caudalis (dexter), 17. N.Vagus, 23. V. jugularis interna, 30. V. subclavia dextra at the junction of V. thyroidea caudalis and V. jugularis interna, 33. Truncus vagosympathicus, 34, 34′ A. carotis communis dextra et sinistra, 36. A. axillaris, 41. Oesophagus, 49. V. thyroidea caudalis, 50. V. cava cranialis. Scale bar = 1 mm.

The N. laryngeus caudalis was the terminal part of N. laryngeus reccurens after giving tracheal and esopheal branches. The N. laryngeus caudalis gave off branches to all of the intrinsic muscles of the larynx except the M. cricothyroideus. The N. laryngeus caudalis entered the glandula thyroidea from the caudal end and terminated in the gland.

4 | DISCUSSION AND CONCLUSION

The location of the glandula thyroidea in Sprague-Dawley rats had previously been reported to be at the level C2-C3 (Hadie et al., 2013). In the present study, we demonstrated that the glandula thyroidea of Wistar Albino rats were localized at the levels of the C1-C2 vertebrae in the rats regardless of their sex. Published studies have also shown that the glandula thyroidea extends to the first three or four trachea rings in mice, and the first four or five in rats (Hebel & Stromberg, 1976; Komârek et al., 2000; Krinke et al., 2000; La Perle et al., 2018; Monroe & Turner, 1946), or can even extend up to the 7th trachea ring (Yavru & Yavru, 1996). It was determined that in the present study the caudal ends of the glandulae thyroidea were at different levels compared to those stated by this previous literature, as they extended to the 3rd or 4th trachea cartilage rings (Figure 10c). In addition, in the present study there was no left lobe in the glandula thyroidea in one female, complimenting previous reports (Alworth & Harvey, 2012; Nakamura et al., 2019).

In one previous study in 8–10 week-old male *Rattus norvegicus*, the glandulae thyroidea measurements were far larger than any other study at 22 × 6 mm, weighing 1.27 g (Sawsan, 2020), which differs greatly in terms of weight compared to other published studies, and was also different to the present research. In rats, the average size reported was previously reported as 7 × 3 × 3 mm, with the glandulae thyroidea weights ranging from 0.013 to 0.028 g (La Perle et al., 2018). Other rat species have shown similar measurements, including 0.0111 g in the large *Neotoma* (*Mexican Pack Rat*), 0.008 g in the medium-sized *Rattus norvegicus* (*Gray Norway Rat*) and 0.00115 g in the small *Dipodomys* (*Kangaroo Rat*) (Crile, 1937; Midgley, 1938). Each glandula thyroidea lobe within the rat measured 3–4 mm

14390264, 0, Downloaded from https://onlinelibrary.wiley.com/doi/10.1111/ahe.12916 by University Of Nottingham, Wiley Online Library on [29/03/2023]. See the Terms and Conditions (https://onlinelibrary.wiley.com/terms-and-conditions) on Wiley Online Library for rules of use; OA articles are governed by the applicable Creative Commons License

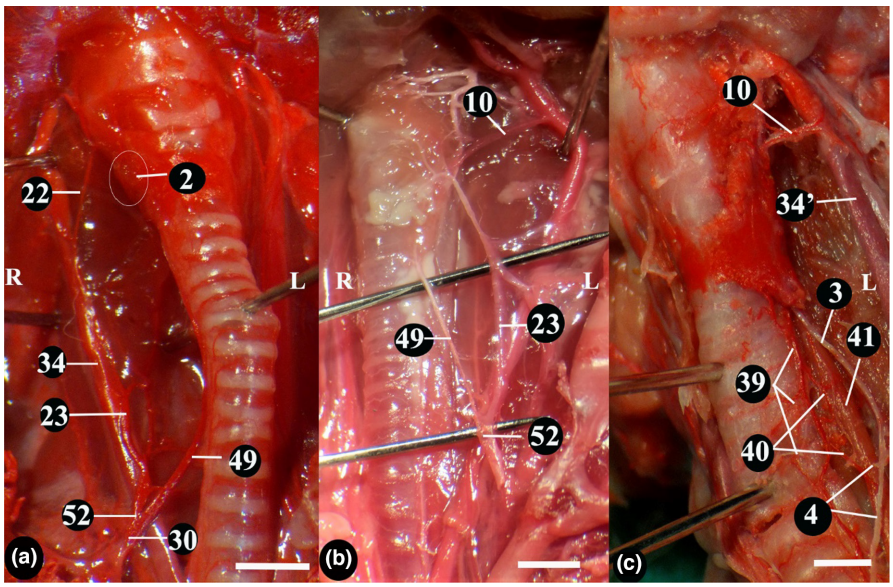

FIGURE 10 Venous drainage and the A. thyroidea caudalis. Ventral views. Male rat. (a, b) Venous drainage of the glandula thyroidea (with latex). (c) A. thyroidea caudalis and its branches. R = Right, L = Left. 2. Glandula parathyroidea, 3. N. Laryngeus caudalis, 4. N. laryngeus reccurens and its oesophageal branch, 10. A. thyroidea cranialis, 22. V. thyroidea cranialis, 23. V. jugularis interna, 30. V. subclavia dextra at the junction of V. thyroidea caudalis and V. jugularis interna, 34, 34′. A. carotis communis dextra et sinistra, 39. A. thyroidea caudalis and its tracheal branches, 40. A. thyroidea caudalis and its oesophageal branches, 41. Oesophagus, 49. V. thyroidea caudalis, 52. The junction place of the V. thyroidea caudalis and the V. jugularis interna. Scale bar = 1 mm.

long, 1.5 mm wide, and weighed approximately 0.005 g (Johanson et al., 1988). According to Hebel and Stromberg (1976), the glandula thyroidea was a pinkish gland on the 4th–5th tracheal rings, 3.9–5.5 mm long, 2–3 mm wide, weighing 0.0154 g in males and 0.0179 g in females. Overall, the measurements from the present study were similar to the majority of the previously published studies, the length of the glandula thyroidea was 4.02–4.34 mm, and the width was between 1.68 and 1.87 mm.

The previously published studies only looked at the combined measurements of the glandulae thyroidea rather than detailed measurements. Therefore, the present study presents novel measurement data of the right and left lobes separately, detailing length, width and depth (thickness) to ensure a more detailed study. It was previously reported that there was a 27% difference in lobe sizes (Nakamura et al., 2019). In our findings, the right lobe measured 4.34 × 1.87 × 0.86 mm in males and 4.02 × 1.68 × 0.80 mm in females, whereas the left lobe was 4.30 × 1.85 × 0.82 mm in males compared to 4.11 × 1.60 × 0.80 mm in females. Therefore, the current study supported that the right and left lobes, in both males and females, were different in size. The present study also analysed male and female glandulae thyroidea measurements individually. The right and left lobe lengths and widths and the right lobe thicknesses were larger in the males compared to females (Table 1; $p < 0.05$), whereas the left lobe did not differ significantly in thickness between males and females.

In the present study, the glandulae thyroidea weights in the 10- to 11-week-old Wistar albino rats were 6.6 ± 3.7 mg in males and 5.5 ± 2.2 mg in females (Table 1; $p = 0.575$) similar to two of the previous studies (Hebel & Stromberg, 1976; La Perle et al., 2018), but providing a more detailed analysis showing a significant overall difference between the sexes.

Both the size measurements and weights of the glandulae thyroidea were highly variable within the published literature, with the Sawsan study (Sawsan, 2020) standing out as different to the present study and other published papers. Other smaller differences in weights and measurements between the studies may be due to differing rat species, ages, weights, variability between researcher measurements and of course potentially differing sexes (especially given any body weight/size differentials between the sexes in the rat). The differences due to sex were not analysed individually within the previous studies; therefore, it is notable that our present study has shown a significant difference between the two. Variability between measurements by differing researchers, and even the precision of the equipment used, is always present between differing research groups. This study reduced intra-observer variables as the measurements were done by one person using the same callipers, but naturally, this cannot reduce the intra-observer variability compared to studies by other groups.

In cats and dogs, the glandulae parathyroideais located anterior or posterior to the glandula thyroidea (Kealy et al., 2010). In the Syrian hamster, it localizes to the anterolateral part of the glandula thyroidea (Kittel et al., 1996b; Pace et al., 2003), measuring approximately 0.7–1 mm × 0.3–0.5 mm in diameter (Kittel et al., 1996b). In mice, the glandula parathyroideais reported as an oval, sometimes longitudinal oval shape (Kittel et al., 1996a), similar to the present findings in the rat. In the present rat study, 60% of the glandulae parathyroidea were located in the cranial part of the lateral lobes, with the remainder localized to the caudal part of the lateral

14390264, 0, Downloaded from https://onlinelibrary.wiley.com/doi/10.1111/ahe.12916 by University Of Nottingham, Wiley Online Library on [29/03/2023]. See the Terms and Conditions (https://onlinelibrary.wiley.com/terms-and-conditions) on Wiley Online Library for rules of use; OA articles are governed by the applicable Creative Commons License

lobes, in a similar location to other species. In this study, in terms of size, the glandula parathyroidea was 1.22×1.02 mm in males and 0.95×0.86 mm in females, similar to a previous report in rats at 1.2–2 mm long and 1.0–1.5 mm wide (Hebel & Stromberg, 1976). In another study, these measurements are larger at 1.29×0.21 mm in females and 1.38×0.33 mm in males (Tadjalli & Faramarzi, 2016). Our study notably showed statistically significant decreases in females compared to males (Table 1; $p < 0.05$).

The isthmus presents as a reasonably wide band of tissue in cows, but in horses, sheep, goats, cats and dogs, it is a narrow tissue remnant and is sometimes absent (Singh & Beigh, 2013; Yamamoto et al., 1995). In the present study, the isthmus presented as a narrow band of tissue and was absent in two female rats, complimenting previous reports (Alworth & Harvey, 2012; Nakamura et al., 2019).

In addition to the locations, size measurements and weights of the glandula thyroidea and the glandula parathyroidea being investigated, the vasculature and innervation of both was also studied in rats. Neural innervation of the glandula thyroidea was not different from that reported in the literature, and therefore supports earlier findings. The normal glandula thyroidea is surrounded by a capsule consisting of a thin layer of connective tissue closely adhered to the outer surface of the gland. This capsule contains blood vessels and nerves, which are most prominent near the poles and the boundary between the lobes and the isthmus. In the rats in the present study, the glandulae thyroidea and the glandulae parathyroidea were surrounded by a thin connective tissue capsule, similar to the previous descriptions provided (Mense & Boorman, 2018). The A. thyroidea cranialis, a branch of the A. carotis externa, supplies the glandula thyroidea, while venous drainage occurs via the V. jugularis interna (Mense & Boorman, 2018). The present study also determined that the gland blood supply was provided via vessels arising from the A. thyroidea cranialis and the A. thyroidea caudalis, with venous drainage conducted via the thyroid veins pouring into the V. jugularis interna. In addition, a strong anastomosis was detected on the dorsal aspect of the trachea between both arteries (Figure 7c).

Yamasaki reported that in rats, the A. thyroidea cranialis originated from the A. carotis externa as a common root with the A. pharyngea ascendens (Yamasaki, 1990). According to our findings, this was the case in five female and six male rats (55% in total), the A. thyroidea cranialis originated with the A. pharyngea ascendens, similar to the previous findings (Yamasaki, 1990). In addition, the A. thyroidea cranialis appeared to be included in the arterial supply of the oesophagus, similar to previous findings in dogs (Swenson et al., 1950). Although it was reported that the dorsal branch of the A. thyroidea cranialis was thicker than the ventral branch (Yamasaki, 1990), the dorsal branch was thinner than the dorsal branch in the present study.

One study previously indicated that the A. thyroidea caudalis could originate from the A. phrenicopericardiaca, the truncus brachiocephalicus, and the subclavian or vertebral arteries (Yamasaki, 1990). However, others have reported that it originates from the truncus costocervicalis on the right side in rats (Green, 1955; Maynard & Downes, 2019). In three female rats studied in the present study, the A. thyroidea caudalis originated as two branches from both the truncus costocervicalis and the A. subclavian dextra on the right side, these branches later joined into a single vessel. In addition, it was determined that it gave branches to the tracheal rings, which has not been stated previously in the literature. Yamasaki also reported that in rats there was no A. thyroidea caudalis on the right side; therefore, nutrition for the glandula thyroidea came from branches of other arteries (Yamasaki, 1990).

The V. thyroidea caudalis vein opened into the V. jugularis interna, but before that, it coursed with the A. thyroidea caudalis and the N. laryngeus reccurens in the *tracheoesophageal sulcus*. The cranial and caudal thyroid veins were joined at the level of the apertura thoracis cranialis on both sides of the neck. Later, as also reported in the literature (Green, 1955; Hadie et al., 2013), it was determined that the thyroid veins connected to the V. subclavia dextra on the right side and the V. cava cranialis on the left side. On the dorsal surface of the trachea, between the lobes of the glandula thyroidea, there was anastomosis evident between the A. thyroidea cranialis and the A. thyroidea caudalis, in line with previous findings (Radlinsky, 2007). Mutuş reported that the pharyngeal veins in rabbits participated in the venous circulation of the larynx (Mutuş, 2001), and Green reported this was undertaken by the pharyngeal plexus veins in rats (Green, 1955). The findings from the present study support those reported by Green (1955). Although size differences between male and female blood vessels and the differing vessels in general are presented in this study, there are important limitations that must be highlighted. Although injection pressure was maintained at a similar pressure for each animal throughout the process, this cannot exclude small differences and may not always represent the differing pressures exerted during differing physiological timepoints in a living animal. These limitations also make it more complex when comparing between differing studies, individual animals or species, or even those with different ages, diseases or pathologies. Despite these complexities, it is still worth investigating the basic measurements of the differing vessels.

In conclusion, although there have been many studies on the rat glandula thyroidea, the present research extends the breadth and depth of knowledge regarding topographic anatomy. Detailed measurements of the glands and vasculature, in-depth dissections, and corrosion casts showing locations and detailing innervation and the courses of blood vessels and nerves, add to the literature. In addition, significant differences in the glandula thyroidea, glandula parathyroidea, isthmus and vasculature measurements existed between males and females. This study has also provided photographic evidence and acts as a useful guide for those wishing to understand the anatomy of the glandula thyroidea, the glandula parathyroidea and their associated structures in the rat.

ACKNOWLEDGEMENTS

The authors would like to thank The University of Nottingham for Open access funding and to thank our universities and departments for supporting our research.

14390264, 0, Downloaded from https://onlinelibrary.wiley.com/doi/10.1111/ahe.12916 by University Of Nottingham, Wiley Online Library on [29/03/2023]. See the Terms and Conditions (https://onlinelibrary.wiley.com/terms-and-conditions) on Wiley Online Library for rules of use; OA articles are governed by the applicable Creative Commons License

CONFLICT OF INTEREST STATEMENT

The authors declare no competing interests.

DATA AVAILABILITY STATEMENT

The data that support the findings of this study are available from the corresponding author upon reasonable request.

ORCID

Ismail Hakki Nur https://orcid.org/0000-0001-7215-8112
William Pérez https://orcid.org/0000-0002-9647-4731
Catrin Sian Rutland https://orcid.org/0000-0002-2009-4898

REFERENCES

Abdreshov, S. N., Akhmetbaeva, N. A., Atanbaeva, G. K., Mamataeva, A. T., & Nauryzbai, U. B. (2019). Adrenergic innervation of the thyroid gland, blood and lymph vessels, and lymph nodes in hypothyroidism. *Bulletin of Experimental Biology and Medicine*, *168*(2), 295–299. https://doi.org/10.1007/s10517-019-04694-8

Allen, E., & Fingeret, A. (2022). *Anatomy, head and neck, thyroid*. StatPearls Publishing.

Alworth, L. C., & Harvey, S. B. (2012). Chapter 39 – Anatomy, physiology, and behavior. In K. A. S. A. R. P. W. M. A. Suckow (Ed.), *The laboratory rabbit, Guinea pig, hamster, and other rodents* (pp. 955–966). Academic Press.

Chiasson, R. B. (1978). *Laboratory anatomy of the white rat* (3rd ed.). WCB Publishers.

Crile, R. (1937). The comparative anatomy of the thyroid and adrenal glands. *Ohio Journal of Science*, *37*(1), 42–61.

Domeij, S. (1990). *The laryngeal mucosa and the superior laryngeal nerve of the rat*. (PhD). Umeå University.

Enemali, F., Hambolu, J., Alawa, J., & Anosike, I. V. (2016). Gross anatomical, histological and histochemical studies of thyroid glands of African Giant rat (*Cricetomys gambianus* Waterhouse, 1840). *IOSR Journal of Pharmacy and Biological Sciences*, *11*, 40–43.

Fox, J., Barthold, S., Davisson, M., Newcomer, C., Quimby, F., & Smith, A. (2007). *The mouse in biomedical research: History wild mice, and genetics* (2nd ed.). Elsevier.

Green, E. C. (1955). *Anatomy of the rat*. Phialdelphia The American Philosophical Society. Hafner Publishing.

Hadie, S., Abdulmanan, H., & Abdullah, S. (2013). Thyroid gland resection in eunthanised rat: A practical guide. *International Medical Journal*, *20*(1), 1–4.

Hall, A. R., & Kaan, H. W. (1942). Anatomical and physiological studies on the thyroid gland of the albino rat. *The Anatomical Record*, *84*(3), 221–239.

Hebel, R., & Stromberg, M. (1976). *Anatomy of the laboratory rat*. The Williams and Wilkins Company.

I.C.V.G.A.N. (2017). *Nomina anatomica veterinaria*. International Committee on Veterinary Gross Anatomical Nomenclature, World Association of Veterinary Anatomists.

Johanson, V., Ofverholm, T., & Ericson, L. E. (1988). A method for selective infusion in the thyroid artery of the rat and mouse. *Acta Endocrinologica*, *119*(1), 37–42. https://doi.org/10.1530/acta.0.1190037

Jones, T., Capen, C., & Mohr, U. (1983). *Monographs on pathology of laboratory animals, endocrine system* (2nd ed.). Springer.

Kealy, K., McAllister, H., & Graham, J. P. (2010). *Diagnostic Radiology and Ultrasonography of the Dog and Cat* (5th ed.,). Saunders Elsevier.

Kittel, B., Ernst, H., & Kamino, K. (1996a). Anatomy, histology, and ultrastructure, parathyroid, mouse. In T. C. Jones, C. C. Capen, & U. Mohr (Eds.), *Endocrine system* (pp. 328–330). Springer Berlin Heidelberg.

Kittel, B., Ernst, H., & Kamino, K. (1996b). Anatomy, histology, and ultrastructure, parathyroid, Syrian hamster. In T. C. Jones, C. C. Capen, & U. Mohr (Eds.), *Endocrine system* (pp. 326–327). Springer Berlin Heidelberg.

Komârek, V., Gembardt, C., Krinke, A., Mahrous, T., & Schaetti, P. (2000). Synopsis of the organ anatomy. In K. G. J (Ed.), *The laboratory rat* (pp. 283–319). Academic Press.

Krinke, G. J. (2004). Normative histology of organs. In H. J. Hedrich & G. Bullock (Eds.), *The laboratory mouse* (pp. 133–166). Academic Press.

Krinke, G. J., Bullock, G., & Tracie, B. (2000). *The laboratory rat (American College of Laboratory Animal Medicine)* (1st ed.). Academic Press.

Kumar, D., Vaish, R., Pandey, Y., Gupta, N., Kumar, U., & Kumar, P. (2018). Thyroid gland: An anatomical perspective. *Journal of Entomology and Zoology Studies*, *6*(4), 1400–1405.

La Perle, K., Marie, D., & Dintzis, S. (2018). Endocrine system. In P. M. Treuting, S. M. Dintzis, & K. S. Montine (Eds.), *Comparative anatomy and histology* (2nd ed., pp. 251–273). Academic Press.

Maynard, R., & Downes, N. (2019). *Anatomy and histology of the laboratory rat in toxicology and biomedical research* (4th ed.,). Academic Press.

McLaughlin, C. A., & Chiasson, R. B. (1990). *Laboratory anatomy of the rabbit* (3rd ed.). Wm. C. Brown.

Mense, M., & Boorman, G. (2018). Thyroid gland. In A. W. Suttie (Ed.), *Boorman's pathology of the rat* (pp. 669–686). Academic press.

Midgley, E. E. (1938). The visceral anatomy of the kangaroo rat. *Journal of Mammalogy*, *19*(3), 304–317.

Monroe, R., & Turner, C. (1946). Thyroid secretion rate of albino rats during growth, pregnancy and lactation. *Research Bulletin: Agricultural Experiment Station*, *304*, 1–34.

Mosier, H. D., & Richter, C. P. (1967). Histologic and physiologic comparisons of the thyroid glands of the wild and domesticated Norway rat. *The Anatomical Record*, *158*(3), 263–274. https://doi.org/10.1002/ar.1091580305

Mota, O., & Serkiz, S. (2019). The comparative anatomy of the thyroid gland in humans and rats. *Bulletin of Problems Biology and Medicine*, *2*(2), 151. https://doi.org/10.29254/2077-4214-2019-2-2-151-210-213

Murakami, T., Hinenoya, H., Taguchi, T., Ohtsuka, A., & Uno, Y. (1987). Blood vascular architecture of the rat parathyroid glands: A scanning electron microscopic study of corrosion casts. *Archivum Histologicum Japonicum*, *50*(5), 495–504. https://doi.org/10.1679/aohc.50.495

Murakami, T., Tanaka, T., Taguchi, T., Ohtsuka, A., & Kikuta, A. (1995). Blood vascular bed and pericapillary space in rat parathyroid glands. *Microscopy Research and Technique*, *32*(2), 112–119. https://doi.org/10.1002/jemt.1070320206

Mutuş, R. (2001). Macroanatomical and morphometric investigation on the maxillary vein in rabbits. *Turkish Journal of Veterinary & Animal Sciences*, *25*, 803–809.

Nakamura, T., Ichii, O., Sunden, Y., Elewa, Y. H. A., Yoshiyasu, T., Hattori, H., Tatsumi, O., Kon, Y., & Nagasaki, K. I. (2019). Slc:Wistar/ST rats develop unilateral thyroid dysgenesis: A novel animal model of thyroid hemiagenesis. *PLoS One*, *14*(8), e0221939. https://doi.org/10.1371/journal.pone.0221939

Nur, I. H. (1992). *Macroanatomical and Subgros studies on the last branches of arteria carotis communis in Akkaraman sheep and angora goat*. (PhD). Selcuk University.

Onwuaso, I. C., & Nwagbo, E. D. (2014). Light and electron microscopic study of thyroid gland in the African giant rat, *Cricetomys gambianus*, waterhouse. *Pakistan Journal of Zoology*, *46*, 1223–1230.

Pace, V., Scarsella, S., & Perentes, E. (2003). Parathyroid gland carcinoma in a Wistar rat. *Veterinary Pathology*, *40*(2), 203–206. https://doi.org/10.1354/vp.40-2-203

Policeni, B. A., Smoker, W. R., & Reede, D. L. (2012). Anatomy and embryology of the thyroid and parathyroid glands. *Seminars in Ultrasound, CT, and MR*, *33*(2), 104–114. https://doi.org/10.1053/j.sult.2011.12.005

14390264, 0, Downloaded from https://onlinelibrary.wiley.com/doi/10.1111/ahe.12916 by University Of Nottingham, Wiley Online Library on [29/03/2023]. See the Terms and Conditions (https://onlinelibrary.wiley.com/terms-and-conditions) on Wiley Online Library for rules of use; OA articles are governed by the applicable Creative Commons License

Radlinsky, M. G. (2007). Thyroid surgery in dogs and cats. *The Veterinary Clinics of North America. Small Animal Practice*, *37*(4), 789–798, viii. https://doi.org/10.1016/j.cvsm.2007.04.001

Romeo, H. E., Gonzalez Solveyra, C., Vacas, M. I., Rosenstein, R. E., Barontini, M., & Cardinali, D. P. (1986). Origins of the sympathetic projections to rat thyroid and parathyroid glands. *Journal of the Autonomic Nervous System*, *17*(1), 63–70. https://doi.org/10.1016/0165-1838(86)90044-5

Sawsan, A. A. (2020). Morphological and histological study on thyroid gland toxicity in male rats exposed to mercury. *Indian Journal of Forensic Medicine & Toxicology*, *14*(4), 2723–2728.

Singh, R., & Beigh, S. A. (2013). Diseases of thyroid in animals and their management. In R. Payan-Carreira (Ed.), *Insights from veterinary medicine*. London, UK.

Stathatos, N. (2019). Anatomy and physiology of the thyroid gland. In L. H. D. A. L. W. M. Luster (Ed.), *The thyroid and its diseases: A comprehensive guide for the clinician* (pp. 3–12). Springer International Publishing.

Swenson, O., Merrill, K., Jr., Peirce, E. C., II, & Rheinlander, H. F. (1950). Blood and nerve supply to the esophagus; an experimental study. *The Journal of Thoracic Surgery*, *19*(3), 462–476.

Tadjalli, M., & Faramarzi, A. (2016). Gross anatomy of the thyroid and parathyroid glands in Indian gray mongoose, (*Herpestes edwardsii*). *Cibtech Journal of Zoology*, *5*(1), 1–5.

Vdoviaková, K., Askin, S., Krešáková, L., Vrabec, V., Vrzgula, M., & Danková, M. (2022). The head and neck vascular anatomical variability in the laboratory rat and its significance to medical science. *Folia Veterinária*, *66*(3), 9–18. https://doi.org/10.2478/fv-2022-0022

Wells, T. (1968). *The rat: A practical guide*. Dover Publications.

Yamamoto, M., Seedor, J. G., Rodan, G. A., & Balena, R. (1995). Endogenous calcitonin attenuates parathyroid hormone-induced cancellous bone loss in the rat. *Endocrinology*, *136*(2), 788–795. https://doi.org/10.1210/endo.136.2.7835311

Yamasaki, M. (1990). Comparative anatomical studies of thyroid and thymic arteries: I. Rat (*Rattus norvegicus albinus*). *The American Journal of Anatomy*, *188*(3), 249–259. https://doi.org/10.1002/aja.1001880304

Yamasaki, M. (1995). Comparative anatomical studies on the thyroid and thymic arteries. III. Guinea pig (*Cavia cobaya*). *Journal of Anatomy*, *186*(Pt 2), 383–393.

Yavru, N., & Yavru, S. (1996). *Deney Hayvanları*. Selçuk Univ. Veteriner Fakultesi Yayınları.

How to cite this article: Nur, I. H., Pérez, W., & Rutland, C. S. (2023). Topographic anatomy and vascularization of the glandula thyroidea in rats. *Anatomia, Histologia, Embryologia*, *00*, 1–12. https://doi.org/10.1111/ahe.12916

14390264, 0, Downloaded from https://onlinelibrary.wiley.com/doi/10.1111/ahe.12916 by University Of Nottingham, Wiley Online Library on [29/03/2023]. See the Terms and Conditions (https://onlinelibrary.wiley.com/terms-and-conditions) on Wiley Online Library for rules of use; OA articles are governed by the applicable Creative Commons License